J Mater Sci (2007) 42:4245–4253
DOI 10.1007/s10853-006-0688-1

Carbon fiber/ceramic matrix composites: processing, oxidation and mechanical properties

Samanta Rafaela de Omena Pina · Luiz Claudio Pardini · Inez Valéria Pagotto Yoshida

Received: 16 March 2006 / Accepted: 19 July 2006 / Published online: 3 March 2007

Abstract Ceramic matrix composites (CMC) have been considered in the last two decades to be alternative materials for highly demanding thermo-structural applications. Pre-ceramic polymers offer significant advantages for manufacturing these composites by the polymer impregnation method. In the present work, carbon fiber/silicon oxycarbide (C/SiC_xO_y) composites were obtained by controlled pyrolysis of carbon fiber/bridge polysilsesquioxane composites (COMPOSITE 1) followed by infiltration/pyrolysis cycles with a polycyclic silicone network. The polysilsesquioxane showed high wettability and adhesion on the carbon fiber surface. An improvement of the thermo-oxidation resistance and a reduction of the porosity as a function of the number of polycyclic silicone infiltration cycles were observed. An extra improvement in the thermo-oxidation protection was found when the C/SiC_xO_y composite was coated with a poly(phenylsilsesquioxane) layer (COMPOSITE 2). Shear properties for the composites showed a dependence on the nature of the matrix. The average in-plane shear strength and the shear modulus were 44.2 ± 1.9 MPa and 2.2 ± 0.5 GPa for the polymeric matrix composite (COMPOSITE 1), respectively. For the ceramic matrix composite (COMPOSITE 2) the values were 14.2 ± 4.1 MPa and 15.0 ± 2.0 GPa, respectively. The properties of the latter composite were also governed by the microstructure of the ceramic matrix.

S. R. de Omena Pina · I. V. P. Yoshida (✉)
Instituto de Química, Universidade Estadual de Campinas – UNICAMP, CP 6154, 13084-971 Campinas, SP, Brazil
e-mail: valeria@iqm.unicamp.br

L. C. Pardini
Centro Técnico Aeroespacial, Instituto de Aeronáutica e Espaço, AMR, 12228-904 São José dos Campos, SP, Brazil

Introduction

Damage tolerance and efficiency enhancement are challenges in aero-engine components and other high temperature industrial devices, such as gas turbines and low weight thermal protection shields. These challenges can be met by using ceramic matrix composites (CMC) [1–4]. Candidates for these materials are mainly based on non-oxide matrixes, such as carbon, SiC, Si_3N_4 or certain oxide matrixes, such as SiC_xO_y, SiO_2–Al_2O_3, etc... [5–10].

Among the preparation methods used for CMC composites, the polymer pyrolysis route is one of the most attractive because it allows the production of complex composite shapes and is cost effective. In addition, any of the conventional processing techniques of the polymeric matrix composite, such as: hand lay-up, autoclave molding, resin transfer molding (RTM) and filament winding can be successfully used to obtain CMC. These methods provide near net shaping for many complex geometries, which is considered to be an advantage in making cost effective parts [5, 8–11].

Silicon-based polymers have received a great deal of attention for their use as pre-ceramic precursors for CMC. Polysilanes, polysiloxanes, polysilazanes and a variety of hybrid polymers containing hetero-atoms,

such as boron, are currently of interest [10–16]. On the other hand, carbon fibers, silicon carbide fibers and alumino-silicate fibers have been used as reinforcement in CMC for highly demanding thermo-mechanical applications [17–19].

The present work focuses on the preparation and characterization of a polymeric matrix composite, obtained from carbon fibers and a bridge polysilsesquioxane matrix precursor by controlled pyrolysis. A polycyclic silicone network generated in situ by the infiltration of a mixture of functional siloxane cyclics and platinum-catalyst, followed by pyrolysis, was used as precursor of SiC_xO_y. After three infiltration/pyrolysis cycles the carbon fiber reinforced ceramic matrix composite was coated with poly(phenylsilsesquioxane) resin in order to enhance its oxidation resistance. The structural evolution of the polymeric matrixes to the corresponding ceramic products was studied. The polymeric and ceramic composites were evaluated by density and porosity measurements, shear tests, thermo-gravimetry and their morphologies were investigated by field emission scanning electron microscopy.

Experimental procedure

Starting raw materials

Plain-weave fabrics made of Toray T300 ex-PAN based carbon fibers were constituted by 3000 filament-count yarns. The polysilsesquioxane matrix (PBFE/APS) was prepared in situ by the reaction between aminopropyltriethoxysilane (APS), $H_2N(CH_2)_3Si(OC_2H_5)_3$, purchased from Aldrich Chemical Company, Inc. (Milwaukee, USA), and an oligomeric epoxy resin derived from polybisphenol A-co-epiclorhydrin (PBFE), Mn ~600 g/mol, supplied by Dow Chemical do Brazil (São Paulo, Brazil).

Commercially available functional siloxane cyclic oligomers, the 1,3,5,7-tetramethyl-1,3,5,7-tetravinylcyclo tetrasiloxane, $[(CH_3)(CH_2{=}CH)SiO]_4$, (D_4Vi), and the 1,3,5,7-tetramethyl-cyclotetrasiloxane, $[(CH_3)(H)SiO]_4$, (D_4H) were supplied by Dow Corning do Brazil (Hortolândia, Brazil). Platinum divinylcomplex, 2–3% in vinyl terminated poly(dimethylsiloxane), (Pt-catalyst) was purchased from Aldrich Chemical Company, Inc. (Milwaukee, USA). These materials were used as received. The mixture of D_4Vi, D_4H and Pt-catalyst was used in the infiltration step with the ceramic matrix composite to produce in situ the polycyclic silicone network as a SiC_xO_y precursor.

Polymeric matrix composite manufacture

Carbon fiber/bridge hybrid polysilsesquioxane composite was made by the hand lay-up technique by stacking 22 layers of carbon fabric impregnated with a mixture of PBFE/APS, in a stoichiometric NH_2:epoxy ratio (1:1). The amine-epoxy addition reaction was followed by the hydrolysis and condensation reactions of alkoxysilane groups, in situ, promoted by environmental moisture.

The bridge hybrid polysilsesquioxane matrix was cured at room temperature and aged for 24 h, to form the green-body laminate polymeric composite, named COMPOSITE 1. Specimens of this composite were trimmed in appropriate dimensions ($4 \times 4 \times 5$ mm) and evaluated by the Iosipescu shear test.

A PBFE/APS monolithic polymeric sample was also obtained as a tough and colorless material, by the same procedure, to study the structural evolution from the polymer to the corresponding ceramic.

Ceramic matrix composite manufacture

Specimens obtained from the green-body laminate (COMPOSITE 1) were pyrolyzed under argon flow with the following heating cycle: heating to 180 °C at 5 °C/min, holding for 60 min at this temperature; heating to 500 °C at 5 °C/min, holding for 60 min at this temperature; and heating to 1000 °C, at 2°C/min, holding for 120 min at this temperature. Finally the specimens were cooled to room temperature at 2 °C/min. These pyrolyzed specimens were named C/C–SiO_2.

In order to obtain CMC with a reasonable density and improved mechanical properties, the C/C–SiO_2 composite samples were infiltrated with a mixture of D_4Vi and D_4H, 58:42 (wt%), respectively, and 0.01 wt% of Pt-catalyst. The polymer was cured at room temperature giving rise to an in situ polycyclic silicone network (DVDH). The composite samples were subsequently pyrolyzed by using the same heating cycle described before. In this step, DVDH was converted to SiC_xO_y. Three infiltration/pyrolysis cycles were carried out, and the corresponding composite samples were named C/SiC_xO_y 1, C/SiC_xO_y 2, and C/SiC_xO_y 3. Finally, the C/SiC_xO_y 3 composite sample was coated with a pre-hydrolyzed phenyltriethoxysilane solution, which gave rise to a thin in situ poly(phenylsilsesquioxane) (POSS) film. This final composite was named COMPOSITE 2 (Fig. 1). To understand the ceramization process, all the composite specimens (COMPOSITE 1, C/C–SiO_2, C/SiC_xO_y 1, C/SiC_xO_y 2, C/SiC_xO_y 3 and COMPOSITE 2) were characterized.

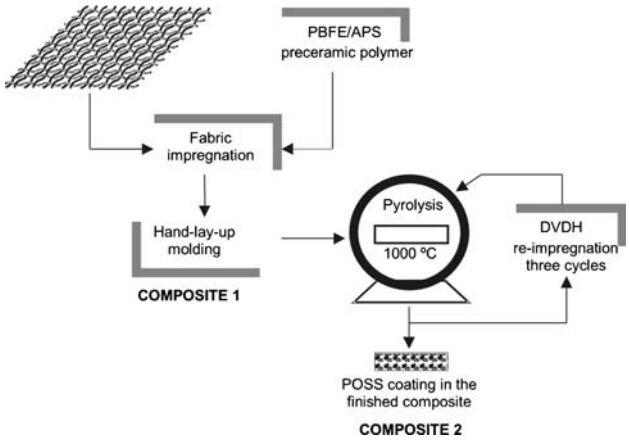

Fig. 1 Schematic diagram of the preparation steps of the composites

Measurement techniques

Monolithic polymeric samples

The structural evolution from polymeric precursors to the corresponding ceramic matrixes was studied on polymeric samples obtained using the same conditions as those used in the preparation of the composites. Infrared spectra (FTIR) were obtained in a Fourier spectrometer (Bomem MB series), operating between 4000 and 400 cm^{-1}, at 4 cm^{-1} resolution, with the conventional transmission KBr pellet technique. ^{29}Si MAS NMR spectra were recorded on a spectrometer (Bruker, model AC300P), operating at 59.62 MHz for ^{29}Si nucleus with a rotation frequency between 3 and 5 kHz. The ^{29}Si one-pulse experiments required a recycle delay of 60 s with 30°-pulse angle. Thermogravimetry (TGA) of the polymeric samples (~10 mg) was performed on a thermo-gravimetric analyzer (2950, TA Instruments) at a heating rate of 20 °C/min from 30 up to 980 °C, in a controlled dry argon flow of 100 mL/min.

Composite samples

The thermo-oxidative behavior of all composite specimens (~10 mg) was studied by thermo-gravimetry in the same equipment as described above, heating from room temperature to 1000 °C at 20 °C/min in a synthetic air flow (Air Liquide: 80% N_2, 20% O_2). The morphology of the composite specimens was analyzed by field emission scanning electron microscopy (FESEM) on a JEOL JSM-6340F equipment after each step of processing, i.e. molding, pyrolysis, infiltration/pyrolysis and coating cycles. For FESEM analyses, rectangular shaped specimens (with $5 \times 5 \times 3.0$ mm) were machined with a band power saw. In order to avoid the direct access of oxygen to the bulk of the carbon fibers in the composites, through the lateral edge, these specimens were trimmed from a COMPOSITE 1 plate and submitted to similar infiltration/pyrolysis cycles as described above, and also to POSS coating procedure. Density measurements of the composites were performed on a picnometer (Micromeritics 1305). The samples were exhaustively purged with He before the measurements. The open porosity of each composite sample (small bars trimmed from the COMPOSITE 1 plate) was characterized by high-pressure mercury intrusion in an Autoscan-33 Quantachrome Porosimeter. The samples were outgassed prior to analysis to facilitate filling of the pores with mercury.

The Iosipescu test

Shear tests were conducted according to the ASTM D 5379 standard [20, 21]. They were performed in an Instron 4301 equipment for both COMPOSITE 1 and COMPOSITE 2. The crosshead speed was 0.5 mm/min. The geometry of the Iosipescu specimen is shown in Fig. 2a. It consists of a beam with two 45° notches machined opposite each other at the mid-point of the specimen. By applying two coupled forces that generate two counter-acting moments, a pure and uniform shear stress state is generated at section ac, between the two notches of the beam. The resulting shear and moment diagrams are shown in Fig. 2b and c, respectively. The maximum average shear stress is calculated by equation 1 [22]:

$$\tau_{xy} = \frac{P}{bt} \tag{1}$$

where P is the load, b is the width between the notches and t is the specimen thickness. The average values of apparent shear stress were taken from measurements on five samples of each polymeric (COMPOSITE 1) and ceramic (COMPOSITE 2) composite. The shear strain was calculated from the strain-gage data by the relationship:

$$\gamma = \varepsilon_1 - \varepsilon_2 \tag{2}$$

where ε_1 and ε_2 are the strains measured by the strain gage elements that are ±45° to the principal material coordinates.

Results and discussion

Carbon fiber polymeric composites are among the strongest materials yet devised, in which the fibers

provide strength and the polymeric matrix allows the fibers to remain together in the correct orientation, protects them from damage, and enables the successive carbon fiber layers to be laminated. In this study, bridge polysilsesquioxane (PBFE/APS) acted as the polymeric matrix. It was prepared from a mixture of epoxy resin and APS, by an addition reaction, as follows:

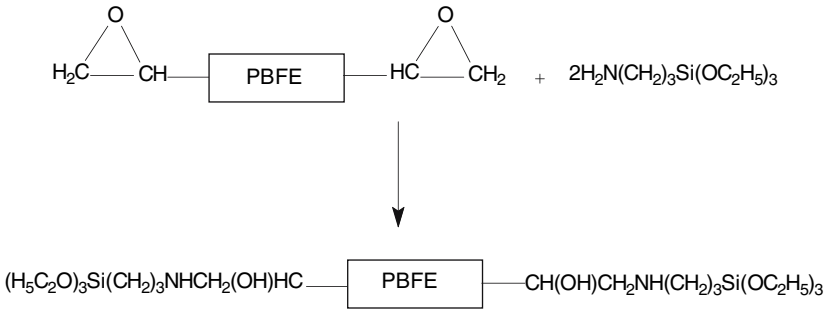

PBFE/APS alkoxysilane showed appropriate properties as a polymeric precursor to intercalate between carbon fiber layers, due to its high wettability and adhesion on the carbon fiber surface. In the presence of environmental moisture, the hydrolysis of Si–OC_2H_5 groups followed by the condensation of Si–OH resulting groups gave rise to the in situ PBFE/APS bridge polysilsesquioxane. Concomitantly to the polycondensation of Si–OC_2H_5 and Si–OH groups, part of these groups can react with C–OH usually present on the carbon fiber surface, by condensation reactions:

These condensation reactions gave rise to a covalent carbon fiber-polymeric matrix interface in COMPOSITE 1. In addition, hydrogen bonds between the carbon fiber surface and the polar O–H and N–H groups, from the polymeric matrix, also contributed to the high adhesion observed between the fiber surface and PBFE/APS bridge polysilsesquioxane matrix.

The pyrolysis of COMPOSITE 1 gave rise to a C/C–SiO_2 composite, which was submitted to three infiltration/pyrolysis cycles with a mixture of (D_4H and D_4Vi) functional cyclic siloxanes and Pt-catalyst. This mixture produced in situ, by a hydrosilylation reaction, the elastomeric polycyclic silicone network named DVDH [23, 24]. The hydrosilylation reaction is an addition reaction, where no by-product is formed [23], as follows:

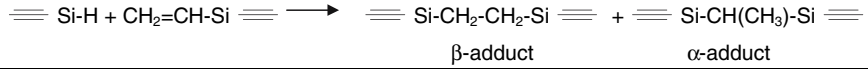

The pyrolysis of DVDH polycyclic silicone at 1000 °C produces a SiC_xO_y residue with a high ceramic yield [24, 25]. TGA curves obtained for each constituent of the composites, in flowing argon, are shown in Fig. 3. The thermal stability, evaluated as a function of the initial weight loss temperature under an argon atmosphere, showed the following order: PBFE/APS < DVDH < carbon fibers. The initial temperature of weight loss, T_i, for PBFE/APS bridge polysilsesquioxane was ~100 °C. The first step of weight loss in this polymer, from ~100 to ~370 °C, was associated with volatile evolution, mainly H_2O and/or ethanol, due to the thermally-induced condensation reactions of residual Si–OH and/or Si–OC_2H_5 groups. T_i for DVDH and carbon fibers were ~470 °C and ~750 °C, respectively. A rapid oxidation of carbon fibers in air begins at temperatures above 500 °C. The ceramic yields in an argon atmosphere at 980 °C, for carbon fibers, DVDH and PBFE-APS were 91.8 ± 0.1, 86.1 ± 0.1 and 25.5 ± 0.1%, respectively. The lower ceramic yield obtained for the polysilsesquioxane is due to the higher organic content in this polymer in relation to DVDH.

The evolution of the molecular structure of the PBFE/APS monolithic polymeric sample as a function of the pyrolysis temperature was investigated by infrared spectroscopy, as shown in Fig. 4. The broad absorption with a maximum in the 1200–1000 cm^{-1} range is due to Si–O–Si stretching and it was observed in all spectra, remaining up to 1000 °C. The broadening and intensification of this band with the increase of the pyrolysis temperature were associated to the Si–O–Si enrichment in the material promoted by loss of the volatile organic groups. Above 200 °C the absorption

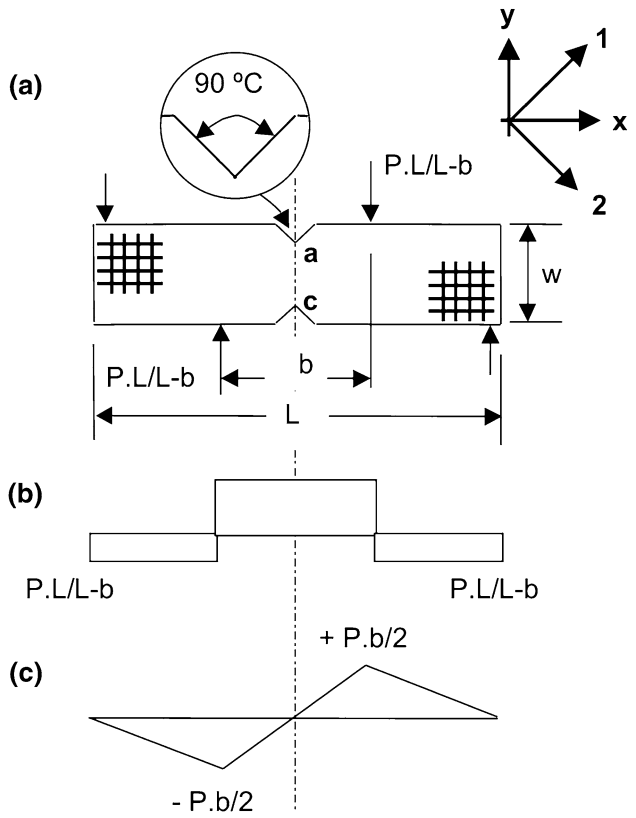

Fig. 2 (**a**) Geometry of the test Iosipescu specimen. (**b**) Shear diagram. (**c**) Moment diagram

at ~480 cm^{-1}, associated with the breath mode of tetrasiloxane ring of the polysilsesquioxane network, band D1, was observed [26–28]. On heating the sample, organic groups were released, promoting the decrease in relative intensities of the absorptions at 2970–2840, 1410 and 1250 cm^{-1}, which are due to aliphatic CH_2 and CH_3 groups, and also at 1600 and 1500 cm^{-1} due to the phenyl rings of the polymeric structure. For the PBFE/APS sample pyrolyzed at 1000 °C, the dark

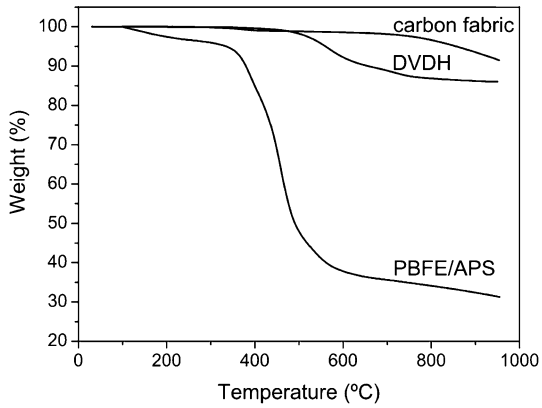

Fig. 3 TGA curves of carbon fabric and polymers used in the preparation of the composites (Ar flow at 20 °C/min)

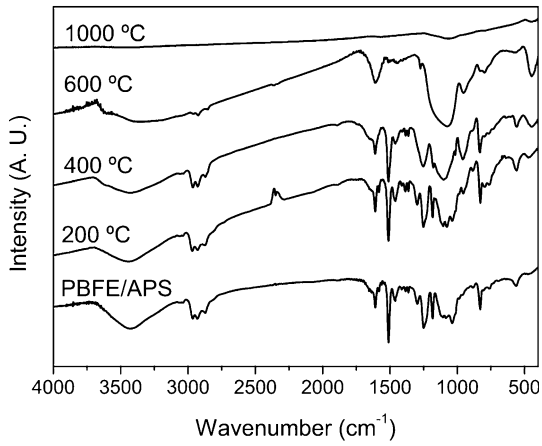

Fig. 4 Infrared spectra of PBFE/APS at different pyrolysis temperatures

residue presented only a very broad and weak absorption, with maximum at ~1080 cm^{-1}, associated with Si–O–Si groups. The low intensity of this absorption suggests the presence of small amount of SiO_2 dispersed in the carbon residue. In addition, absorptions of the carbon phase that are very weak in the infrared [10, 24, 25], were not observed.

The structural evolution of DVDH to the ceramic phase as a function of the pyrolysis temperature can be observed in Fig. 5. Absorptions at 3055 and 1610 cm^{-1} are characteristic of vinyl residual groups, corresponding to C–H and C=C stretchings, respectively. The strong band at 2160 cm^{-1} is typical of Si–H stretching [10, 23, 24], which suggests the presence of residual Si–H groups in the polymeric precursor. As can be seen, practically all the C=C groups were consumed at 400 °C, indicating the increase in the degree of connection between the siloxane cycles at this

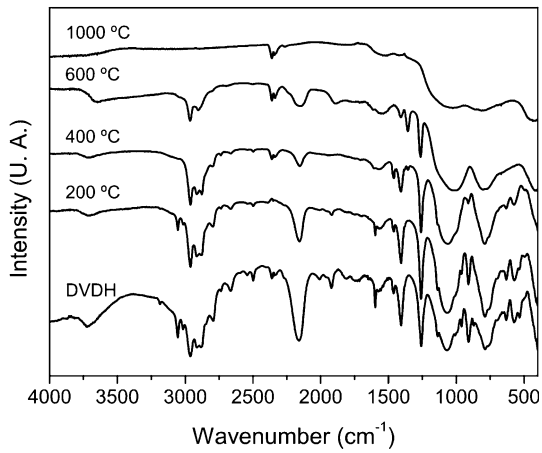

Fig. 5 Infrared spectra of DVDH polycyclic silicone network at different pyrolysis temperatures

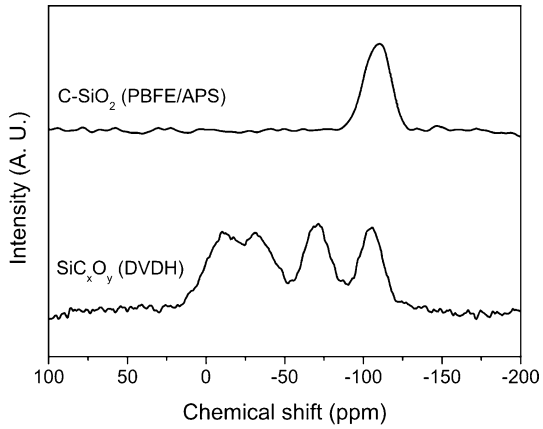

Fig. 6 ^{29}Si MAS NMR spectra of the ceramic residues derived from the pyrolysis of PBFE/APS and DVDH at 1000 °C under Ar flow

temperature. Residual amounts of Si–H groups still were detected in the product up to 600 °C. As described by Schiavon et al. [24], after the consumption of Si–H groups by thermal induced hydrosilylation, they are generated by reorganization reactions of siloxane chains during pyrolysis. Between 200 and 600 °C, the decreases in the relative intensities of the aliphatic C–H absorptions in the 2960–2890 cm^{-1} range and at 1263 cm^{-1} was significant, suggesting that the mineralization of the DVDH polymeric network started around 600 °C. Two broad bands centered at 1080 and 800 cm^{-1} were assigned to Si–O–Si and Si–C stretchings, respectively, in the sample pyrolyzed at 1000 °C under an inert atmosphere. The spectrum of this sample showed a profile characteristic of a carbidic-rich SiC_xO_y ceramic [24].

The ceramic matrixes obtained from PBFE/APS and DVDH polymers by pyrolysis at 1000 °C were also characterized by ^{29}Si MAS NMR, as shown in Fig. 6. The ceramic product derived from PBFE/APS showed only a broad peak centered at –108 ppm, associated to SiO_4 sites, characteristic of silica (SiO_2). This resulting silica was dispersed in a rich carbon phase [25]. For DVDH, the spectrum showed peaks at –106, –72, –32, –16 and 5 ppm, associated with a random distribution of SiO_4, SiO_3C, SiO_2C_2, SiC_4 and $SiOC_3$ sites in the SiC_xO_y residue, respectively [10, 23, 24, 29]. In addition to this, a high abundance of SiC_4, compared to usual ceramic products obtained from the pyrolysis of alkoxysilane gels, was also observed [24, 26, 30–32].

The apparent densities and porosities of the composites at various stages of the preparation process are given in Table 1. The pyrolysis of COMPOSITE 1 led to the formation of the C/C–SiO_2 sample, which showed cracks and pores caused by the evolution of a high amount of organic volatiles from the PBFE/APS polymeric phase. However, the apparent density increased due to volume contraction. The subsequent infiltration/pyrolysis cycles contributed to an increase in the density values and a decrease in the porosity, due to enrichment in the SiC_xO_y ceramic phase. In fact, this behavior was applied to C/SiC_xO_y 1 and C/SiC_xO_y 2 composites. A distinct behavior was found for the C/SiC_xO_y 3 composite, due to the coalescence of closed and isolated pores generating areas with open porosity. In COMPOSITE 2 the thin layer of POSS polymeric film reduced considerably the porosity by filling the pores and also contributed to a slight decrease in the density value of this composite.

Table 1 Apparent density and porosity of the composites

Composites	Apparent density [g cm^{-3}]	Porosity [%]
COMPOSITE 1	1.50	3.2
C/SiO_2	1.59	19.0
C/SiC_xO_y 1	1.75	7.0
C/SiC_xO_y 2	1.82	3.5
C/SiC_xO_y 3	1.80	4.5
COMPOSITE 2	1.76	3.0

The thermo-oxidation experiments were carried out up to 1000 °C in the TGA oven under a synthetic air-flow. The results are shown in Fig. 7. COMPOSITE 1 showed its temperature of maximum degradation rate, T_d, at 840 °C, with a ~5% residue at 1000 °C. The C/C–SiO_2 composite showed a better thermo-oxidative performance than the former. In addition, the introduction of the SiC_xO_y phase by infiltration/pyrolysis cycles of DVDH polycyclic silicone (C/SiC_xO_y 1, C/SiC_xO_y 2 and C/SiC_xO_y 3) led to an increase in T_d values, in relation to the former, due to the effective protection by SiC_xO_y of the carbon fibers with respect to oxygen diffusion. Similar results were described by

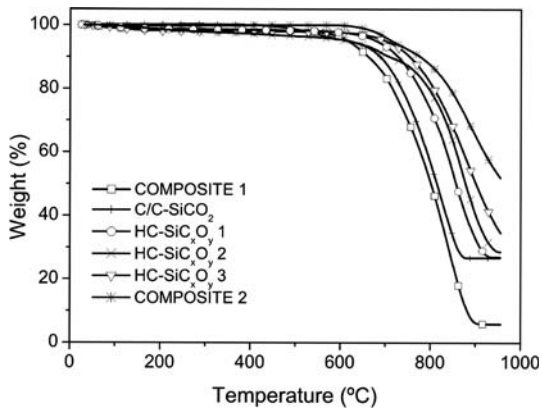

Fig. 7 TGA curves under synthetic air-flow for all composites

Manocha et al. [33] in SiC_xO_y-coated carbon fibers. COMPOSITE 2 showed T_d at ~890 °C and a ~53% residue at 1000 °C. This result also reflects the remarkable effect of the poly(phenylsilsesquioxane) coating layer, as an additional barrier to oxygen diffusion into the composite.

Figure 8 shows SEM micrographs of polymeric and ceramic composites. Good adhesion at the PBFE/APS polymeric matrix/carbon fiber interface was observed in COMPOSITE 1, as can be seen in Fig. 8a. Figure 8b illustrates typical pores in the C/C–SiO_2 composite produced by organic volatile evolution during the pyrolysis of the PBFE/APS polymeric phase. The porosity in the subsequent composites was significantly reduced due to the presence of the SiC_xO_y phase formed by infiltration/pyrolysis cycles of the DVDH polycyclic silicone network. A good adhesion of this ceramic phase on the carbon fiber surface was also observed, as can be seen in Fig. 8c–e, even considering the possible mechanical damages promoted by the power saw in the preparation step for these samples. Little fractures in the matrix phase surface and at the fiber-matrix interface may have been mechanically generated during the cutting of the samples due to saw vibration. In order to seal the remaining pores in the C/SiC_xO_y 3 composite, a further coating with a POSS layer was made. The micrograph of this coated composite surface (COMPOSITE 2) revealed that a uniform thin POSS layer, with a very smooth surface, was formed on the analyzed specimen (Fig. 8f). In this composite the carbon fibers and ceramic phase were shielded by a POSS layer.

Tests for measuring shear strength and modulus of composites have been used in the characterization of composites [20, 22, 34–37]. In these tests the main difficulty is to assure a nearly pure shear stress state in the gage section of the specimen at a constant magnitude. In fiber-reinforced composites there is an additional difficulty related to the orientation of fibers. Unlike with isotropic materials, when measuring composite properties it is necessary to point out the plane where the load is being applied, and the orientation of the

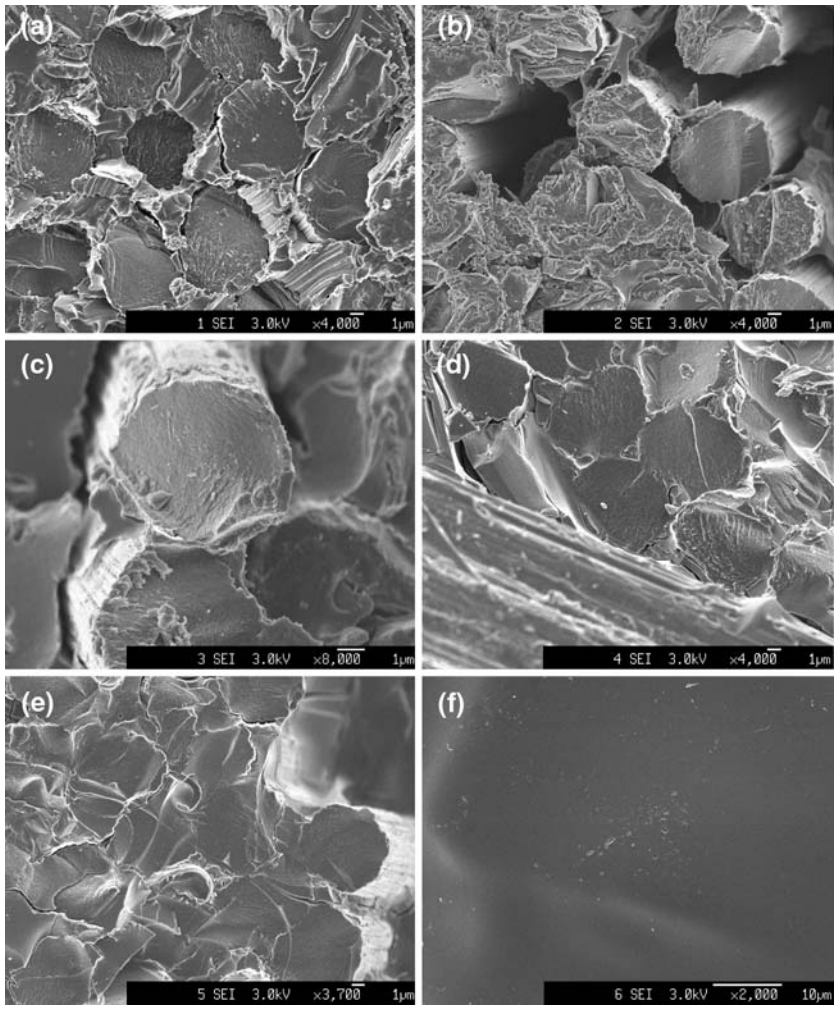

Fig. 8 FESEM micrographs of polymeric and ceramic composites: (**a**) COMPOSITE 1; (**b**) C/C–SiO_2; (**c**) C/SiC_xO_y 1; (**d**) C/SiC_xO_y 2; (**e**) C/SiC_xO_y 3, and (**f**) COMPOSITE 2

fiber axis in relation to the applied load. Only in 1992, the V-notch Iosipescu test was established as a standard procedure for shear testing [34]. In this investigation, a direct comparison of the shear test results between COMPOSITE 1 and COMPOSITE 2 is obviously inappropriate since their matrixes are different. These composites were prepared by stacking *Plain* weave fabric layers and counter-reacting forces were applied, as shown in Fig. 2. Considering the axis system for the test specimen, the shear modulus to be measured is G_{xy}. For COMPOSITE 1 (carbon fiber/PBFE/APS polymeric matrix) the average in-plane shear strength and the shear modulus were 44.2 ± 1.9 MPa and 2.2 ± 0.5 GPa, respectively. For comparison, the shear strength of an epoxy resin specimen measured by torsion can vary from 40 to 90 MPa, depending on the rate of loading [35]. The in-plane shear strength and shear modulus for laminate composites is highly dependent on the matrix and interfacial properties. Similar values of the shear strength and shear modulus were also described by Odegard and Kumosa [36] and Chiang and Jianmei [37], respectively. Figure 9 shows a typical stress-strain curve of the Iosipescu shear test for COMPOSITE 1. The curve shows a typical non-linear behavior up to failure shear stress. For composites having reinforcing fibers perpendicular to the shear loading direction, the failure mode occurs mainly by fiber slipping and debonding at the fiber/matrix interface, as schematically represented in Fig. 10a. On the other hand, in composites having reinforcing fibers parallel to the shear loading direction, the failure may occur by an interlaminar crack at the sample gage length, as schematically represented in Fig. 10b. In any case, shear properties are mainly dominated by the matrix and the fiber/matrix interface and the failure modes are associated with a shear deformation mechanism. For COMPOSITE 1, which is made with a *Plain* weave fabric, there is an additional failure mechanism, besides fiber/matrix interface slipping and interlaminar shear, associated with the fiber bundle splitting in the fabric mesh, as shown schematically in Fig. 10c.

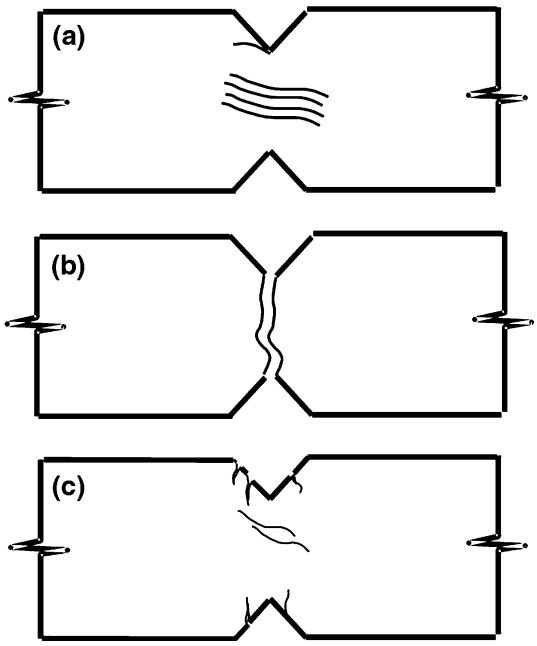

Fig. 10 Representation of main failure modes found in the Iosipescu shear testing

Figure 11 shows a typical stress-strain curve of the Iosipescu shear test for COMPOSITE 2 (C/SiC_xO_y 3/POSS). The average shear strength and shear modulus for COMPOSITE 2 were 14.2 ± 4.1 MPa and 15.0 ± 2.0 GPa, respectively. Non-linearity was observed to a minor extent and the deformation level up to failure was low (~0,2%). Similar results for shear strength were found by Durán et al. [38] in C/SiC composites having 10% porosity. In addition, Bröndsted et al. [39]

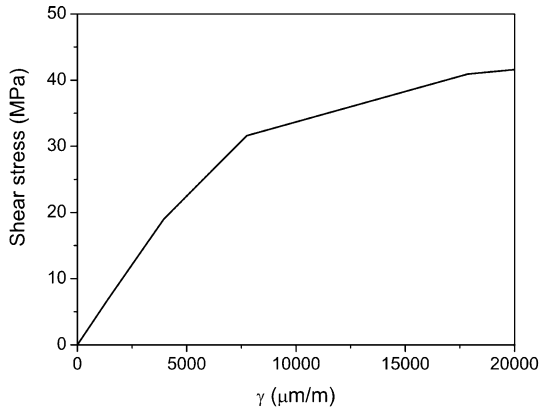

Fig. 9 Typical shear stress curve as a function of shear strain for the polymeric composite

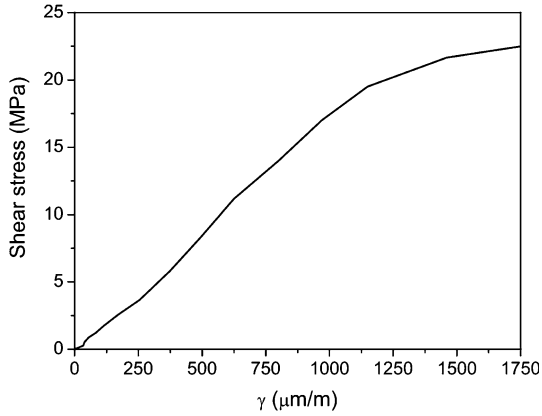

Fig. 11 Typical shear stress curve as a function of shear strain for the ceramic composites

described similar values for the in-plane shear modulus for a C/SiC composite. Apart from the shear failure mechanisms described for polymeric matrix composites, the shear behavior of CMC, as in the case of COMPOSITE 2, is also influenced by the presence of pores and microcracks in the bulk matrix and at the fiber/matrix interface. These features can explain the low shear strength found in these latter composites. Due to the fragile nature of the CMC, the failure in COMPOSITE 2 occurred at the gage section of the specimen, as represented in Fig. 10b, and the scatter of the experimental data is relatively high.

Conclusions

Bridge polysilsesquioxane produced by the in situ reaction between an epoxy resin (PBFE) and APS was an excellent polymeric matrix to produce carbon fiber-reinforced polymeric composites (COMPOSITE 1), due to the high adhesion at the fiber-polymer interface. The pyrolysis of this polymeric composite followed by further infiltration/pyrolysis cycles with a DVDH polycyclic silicone network, led to a progressive increase in the apparent density and in the thermo-oxidation resistance of the ceramic composites, due to SiC_xO_y enrichment of the ceramic phase. In addition, a good adhesion between carbon fibers and the ceramic phase was observed. The highest thermo-oxidative resistance was found for the ceramic composite coated with poly(phenylsilsesquioxane), named COMPOSITE 2. Shear properties (strength and modulus) obtained by the Iosipescu method for COMPOSITES 1 and 2 showed a dependence on the nature of the matrix. The average in-plane shear strength and shear modulus were 44.2 ± 1.9 MPa and 2.2 ± 0.5 GPa for the polymeric matrix composite (COMPOSITE 1), respectively. For the ceramic matrix composite (COMPOSITE 2) the values were 14.2 ± 4.1 MPa and 15.0 ± 2.0 GPa, respectively. Additionally, for the last composite these properties seemed to be governed by the microstructure of the ceramic matrix. Failure modes observed for the composites were described by a shear deformation mechanism.

Acknowledgments We gratefully acknowledge financial support from CNPq and FAPESP (Process 00/06882-5).

References

1. Wang C, Zhu Z, Hou X, Li H (2000) Carbon 38:1821
2. Erauzkin E, Llorca J (1997) Key Eng Mater 127:761
3. Wilshire B, Carreño F (2000) J Euro Ceram Soc 20:463
4. Ohnabe H, Masaki M, Onozuka M, Miyahara M, Sasa T (1999) Compos Part A Appl Sci Manuf 30:489
5. Mckee DW (1987) Carbon 25:551
6. Eherburger P, Lahaye J (1981) Carbon 19:7
7. Manoucha LM (1994) Carbon 32:213
8. Zhou X, Zhang C, Ma J, Zhou A (1999) Key Eng Mater 164:43
9. Shimoo T, Okamura K, Toyoda F (2000) J Mater Sci 35:3811
10. Radovanovic E, Gozzi MF, Gonçalves MC, Yoshida IVP (1999) J Non-Cryst Solids 248:37
11. Wonderly C, Grenestedt J, Ferlung G, E Cepus (2005) Compos Part B Eng 36:417
12. Gozzi MF, Gonçalves MC, Yoshida IVP (1999) J Mater Sci 34:155
13. Schiavon MA, Sorarù GD, Yoshida IVP (2002) J Non-Cryst Solids 304:76
14. Schiavon MA, Sorarù GD, Yoshida IVP (2004) J Non-Cryst Solids 348:156
15. Greil P (1995) J Am Ceram Soc 78:835
16. Kaindl A, Lehner W, Greil P, Kim DJ (1999) Mater Sci Eng A Struct 260:101
17. Krenkel W, Heidenreich B, Renz R (2002) Adv Eng Mater 4:427
18. Davies IJ, Hamada H (2001) Adv Compos Mater 10:77
19. Twitty A, Russellfloyd RS, Cooke RG, Harris B. (1995) J Eur Ceram Soc 15:455
20. ASTM D5379-93 (1993) In Standard method for shear properties of composite materials by the V-notched beam method. American Society for the Testing of Materials, New York
21. Iosipescu N (1967) J Mater 2:537
22. Tarnopo'skii YM, Arnautov AK, Kulakov AVL (1999) Compos Part A Appl Sci Manuf 30:879
23. Redondo SUA, Radovanovic E, Torriani IL, Yoshida IVP (2001) Polymer 42:1319
24. Schiavon MA, Radovanovic E, Yoshida IVP (2002) Powder Technol 123:232
25. Schiavon MA, Redondo SUA, Pina SRO, Yoshida IVP (2002) J Non-Cryst Solids 304:92
26. Li X, King TA (1996) J Non-Cryst Solids 204:235
27. Bornhauser P, Calzaferri G (1996) J Phys Chem 100:2035
28. Bellamy LJ (1966) In The infrared spectra of complex molecules, Methuen, London
29. Hurwitz FI, Kacik TA, Bu XY, Masnovi J, Heimann PJ, Beyene K (1995) J Mater Sci 30:3130
30. Belot V, Corriu RJP, Leclerq D, Mutin PH, Vioux A (1992) J Non-Cryst Solids 144:287
31. Renlund GM, Prochaska S, Doremus RH (1991) J Mater Res 6:2716
32. Pantano CG, Singh AK, Zhang H (1999) J Sol-Gel Sci Technol 14:7
33. Manocha LM, Manocha S, Patel KB, Glogar P (2000) Carbon 38:1481
34. Liu JY (2000) In Shear test fixture design for orthotropic materials, International Community for Composite Engineering, Denver, ICCE/7
35. Gilat A, Goldberg RK, Roberts GD (2005) In Strain rate sensitivity of epoxy resin in tensile and shear loading, NASA/TM, 2005-213595
36. Odergard G, Kumosa M (2000) Compos Sci Technol 60:2917
37. Chiang MYM, Jianmei H (2002) Compos Part B Eng 33:461
38. Durán A, Aparicio M, Rebstock K, Vogel W (1997) Key Eng Mater 127:287
39. Bröndsted P, Heredia FE, Evans AG (1994) J Am Ceram Soc 77:2569